

Empirical Emission Functions for LPM Suppression of Photon Emission from Quark-Gluon Plasma

S. V. S. Sastry

Nuclear Physics Division, Bhabha Atomic Research Centre, Trombay, Mumbai 400 085, India

Abstract

The LPM suppression of photon emission rates from the quark gluon plasma have been studied at different physical conditions of the plasma given by temperature and chemical potentials. The integral equation for the transverse vector function ($\tilde{\mathbf{f}}(\tilde{\mathbf{p}}_\perp)$) consisting of multiple scattering effects is solved by the variational method as well as the self consistent iterations method for the parameter set $\{p_\parallel, k, \kappa, T\}$, for bremsstrahlung and **aws** processes. The peak positions of these ($\tilde{\mathbf{f}}(\tilde{\mathbf{p}}_\perp)$) distributions for the set $\{p_\parallel, k, \kappa, T\}$ depend only on the dynamical variable x defined by, $x = \frac{T}{\kappa_0} \left| \frac{1}{p_\parallel} - \frac{1}{p_\parallel + k} \right|$. The integration over these distributions multiplied by x^2 factor is also shown to depend on this variable x , leading to a *unique global function* $g(x)$ for all temperatures and chemical potentials. Empirical fits to this *dimensionless emission function*, $g(x)$, are obtained. The photon emission rate calculations with LPM suppression effects reduce to one dimensional integrals that involve folding over the empirical $g(x)$ function with appropriate quark distribution functions and the kinematic factors. Using this approach, the suppression factors for both bremsstrahlung and **aws** have been estimated for various chemical potentials and compared with results of rigorous calculations using variational method. It has been found that the k/T is good scale for suppression factors only for zero density case. At finite density the bremsstrahlung and **aws** suppression factors versus k/T are temperature dependent.

Photons production is known to be an important signal of the quark gluon plasma formation (QGP) expected in the relativistic heavy ion collisions. Photons are emitted at various stages during plasma evolution and for an overview one may see [1] and the references therein. The processes of bremsstrahlung and **aws** arise at effective two loop level and contribute at the leading order $O(\alpha\alpha_s)$ owing to the collinear singularity that is regularized by the effective thermal masses [2]. The higher order multiple scatterings may also contribute at the same order as the one and two loop processes [3, 4, 5, 6, 7, 8]. Further, multiple soft scatterings of the fermion during photon emission reduce the emitted photon coherence lengths, known as Landau-Pomeranchuk-Migdal (LPM) effect. The photon emission rates are suppressed owing to the LPM effects [4, 6, 7], especially as shown by the suppression factors in Fig. 7. of [7]. It has been shown that the bremsstrahlung radiation is strongly suppressed to almost 20% at very low k/T values, whereas the photon emission from **aws** falls strongly for higher k/T values [7]. Thus the LPM suppression affects opposite ends of the photon emission spectrum for bremsstrahlung and **aws** processes.

The photon production rates from bremsstrahlung and the **aws** processes have been estimated in [2], in terms of simple one dimensional momentum integrals and the dimensionless quantities J_T, J_L . The J_T and J_L weakly depend on the thermal masses, only through m_g^2/m_∞^2 [2] and therefore are not very sensitive to temperature and the chemical potentials. The photon (energy k_0) differential emission rate per unit volume without and with LPM effects are given by \mathcal{R}^0 and \mathcal{R} respectively.

$$\mathcal{R}_{b,a}^0 = C_k \int dp \left[p^2 + (p+k)^2 \right] [n_B(k_0)(n_f(p) - n_f(p+k))] (J_T - J_L) \quad (1)$$

$$\mathcal{R}_{b,a} = \frac{80\pi T^3 \alpha_s}{(2\pi)^3 9\kappa} \int dp_{\parallel} \left[\frac{p_{\parallel}^2 + (p_{\parallel} + k)^2}{p_{\parallel}^2 (p_{\parallel} + k)^2} \right] \left[n_f(k + p_{\parallel})(1 - n_f(p_{\parallel})) \right] \int \frac{d^2 \mathbf{p}_{\perp}}{(2\pi)^2} 2\tilde{\mathbf{p}}_{\perp} \cdot \Re \tilde{\mathbf{f}}(\tilde{\mathbf{p}}_{\perp}) \quad (2)$$

In the above $C_k = \frac{40\alpha_s T}{9\pi^4 k^2}$ and $\kappa = m_{\infty}^2/m_D^2$ ($\kappa_0 = \frac{1}{4}$ for $\mu = 0$ case). The subscripts (b, a) are for bremsstrahlung and **aws** with different kinematic domains and appropriate distribution functions. κ depends on the physical condition of the plasma such as temperature, baryon density, quark and gluon fugacities and is determined by the thermal mass ratios. In this work we consider a two flavor three color case with $\alpha_s = 0.2$.

$\Re \tilde{\mathbf{f}}(\tilde{\mathbf{p}}_{\perp})$ in Eq. 2 is the real part of a transverse vector function which consists of the LPM effects due to multiple scatterings. This can be taken as transverse momentum vector ($\tilde{\mathbf{p}}_{\perp}$) times a scalar function of transverse momentum \tilde{p}_{\perp} . The sign \sim denotes the dimensionless quantities in units of Debye mass m_D as defined in [7]. The function $\tilde{\mathbf{p}}_{\perp} \cdot \Re \tilde{\mathbf{f}}(\tilde{\mathbf{p}}_{\perp})$ is determined by the collision kernels ($\tilde{C}(\tilde{\mathbf{q}}_{\perp})$) in terms of the following integral (AMY) equation as derived by Arnold, Moore and Yaffe (for details see [7]).

$$2\tilde{\mathbf{p}}_{\perp} = i\delta\tilde{E}(\tilde{\mathbf{p}}_{\perp}, p_{\parallel}, k)\tilde{\mathbf{f}}(\tilde{\mathbf{p}}_{\perp}, p_{\parallel}, k) + \int \frac{d^2 \tilde{\mathbf{q}}_{\perp}}{(2\pi)^2} \left[\tilde{\mathbf{f}}(\tilde{\mathbf{p}}_{\perp}, p_{\parallel}, k) - \tilde{\mathbf{f}}(\tilde{\mathbf{p}}_{\perp} + \tilde{\mathbf{q}}_{\perp}, p_{\parallel}, k) \right] \tilde{C}(\tilde{\mathbf{q}}_{\perp}) \quad (3)$$

$$\tilde{C}(\tilde{\mathbf{q}}_{\perp}) = \kappa \int d\tilde{q}_{\parallel} d\tilde{q}^0 \delta(\tilde{q}^0 - \tilde{q}_{\parallel}) \frac{1}{\tilde{q}} \left[\frac{2}{|\tilde{q}^2 - \tilde{\Pi}_L(\tilde{q}^0, \tilde{q})|^2} + \frac{(1 - (\tilde{q}^0/\tilde{q})^2)^2}{|(\tilde{q}^0)^2 - \tilde{q}^2 - \tilde{\Pi}_T(\tilde{q}^0, \tilde{q})|^2} \right] \quad (4)$$

$$\delta\tilde{E}(\tilde{\mathbf{p}}_{\perp}, p_{\parallel}, k) = \frac{kT}{2p_{\parallel}(k + p_{\parallel})} \left[\tilde{p}_{\perp}^2 + \kappa \right] \quad (5)$$

Aurenche, Gelis and Zaraket obtained an analytical form for the collision kernel in Eq. 44 of [5] by establishing sum rules for the thermal gluon spectral functions. We used this AGZ kernel in the present work.¹ We solved the integral equation for the $\tilde{\mathbf{p}}_{\perp} \cdot \Re \tilde{\mathbf{f}}(\tilde{\mathbf{p}}_{\perp})$ for the set of $\{p_{\parallel}, k, \kappa, T\}$ values using both variational method and some test cases by self consistent iterations. The present study includes nine different chemical potential values from 0-2GeV in steps of 0.25GeV representing baryon density and for each density case at five temperatures of $T=0.25, 0.35, 0.45, 0.55$ GeV. Additional two cases of quark and gluon fugacities representing unsaturated phase space at $T=0.55$ GeV were studied. The photon energy was binned into twenty five values for $k/T = 0.0 - 20.0$ whereas the p_{\parallel} is the integration variable. As mentioned in [9], the variational parameter A_v was not optimised. This is taken from an empirical expression given below as predicted by results of iterations. The β and C_t parameters were found to vary weakly with temperature. As shown in [9] the A_v values are taken to be independent of chemical potentials, together with $\beta = -0.62$ and $C_t = 1.0$ for both bremsstrahlung and **aws** processes.

$$A_v(p_{\parallel}, k) = C_t \left(\frac{T}{\kappa_0} \left| \frac{1}{p_{\parallel}} - \frac{1}{p_{\parallel} + k} \right| \right)^{\beta} \quad (6)$$

The results of rigorous variational calculations for all the cases of the set of $\{p_{\parallel}, k, \kappa, T\}$ have been analyzed for empirical understanding. It has been observed that the $\tilde{\mathbf{f}}(\tilde{\mathbf{p}}_{\perp})$ distributions and therefore their peak positions are not very sensitive to the chemical potentials. It should be noted that even for the cases when the A_v values of the variational parameter deviate from the

¹My earlier reported anomaly of kernel near $\tilde{p}_{\perp} \sim 0$ [9] was due to a numerical problem. It was pointed out by Dr. Francois Gelis together with the possible source of error. The error was corrected and the calculations of [9] were repeated with exact AGZ kernel and the results were not much affected. I thank Dr. Gelis for this important correction.

exact peak position of these distributions, the variational method with large trial set still gives correct results. Peak search has been performed and peak position values of these distributions are obtained. Figure 1 shows the peak position values of these $\tilde{\mathbf{p}}_{\perp} \cdot \Re \tilde{\mathbf{f}}(\tilde{\mathbf{p}}_{\perp})$ distributions plotted as a function photon energies for all p_{\parallel} for each k . The symbols (b,a) in the curve labels in figure are for the bremsstrahlung and **aws** processes and the temperature values shown in figure labels. It can be seen that these peak positions vary strongly with both p_{\parallel} and k independently and are process dependent.

It is interesting to note that the variational parameter depends only on the dimensionless scale $x = \frac{T}{\kappa_0} \left| \frac{1}{p_{\parallel}} - \frac{1}{p_{\parallel}+k} \right|$. This is perhaps expected as the AMY equation depends only on the scale x rather than p_{\parallel} and k independently. Therefore in Figure 2, we plotted the peak position values corresponding to all cases in Fig. 1 versus the new scale x . It can be seen that the strong p_{\parallel} and k dependence has almost merged into a single curve, establishing that x is the only relevant dynamical scale. It suggests that it is sufficient to study the integral equation for the set $\{x, T\}$ rather than for $\{p_{\parallel}, k, \kappa, T\}$. The agreement of the (variational method) data in Fig. 2 can be improved by suitable temperature dependent factors. In the following, we study the new dynamical scale in more detail. For this purpose we rewrite the Eq. 2 by a rearrangement of terms as given below.

$$\mathcal{R}_{b,a} = \mathcal{C}_k \int dp_{\parallel} \left[p_{\parallel}^2 + (p_{\parallel} + k)^2 \right] \left[n_f(k + p_{\parallel})(1 - n_f(p_{\parallel})) \right] C_g g(p_{\parallel}, k, \kappa, T) \quad (7)$$

$$g(p_{\parallel}, k, \kappa, T) = \left(\frac{\kappa_0}{\kappa} \right)^{0.40} \left[\frac{kT/\kappa_0}{p_{\parallel}(p_{\parallel} + k)} \right]^2 \int \frac{d^2 \mathbf{p}_{\perp}}{(2\pi)^2} 2\tilde{\mathbf{p}}_{\perp} \cdot \Re \tilde{\mathbf{f}}(\tilde{\mathbf{p}}_{\perp}) \quad (8)$$

$$= g(p_{\parallel}, k, \kappa, T) = \left(\frac{\kappa_0}{\kappa} \right)^{0.40} x^2 \int \frac{d^2 \mathbf{p}_{\perp}}{(2\pi)^2} 2\tilde{\mathbf{p}}_{\perp} \cdot \Re \tilde{\mathbf{f}}(\tilde{\mathbf{p}}_{\perp}) \quad (9)$$

$$C_g = \frac{\kappa}{T} \left(\frac{\kappa_0}{\kappa} \right)^{-0.40}$$

In these equations, the multiplicative function \mathcal{C}_k is same as the factor appearing in Eq. 1. C_g is the density and temperature dependent coefficient. The new function $g(p_{\parallel}, k, \kappa, T)$ contains the LPM suppression effects and any non trivial κ, T dependence. Using the results from the variational method, we have calculated the $g(p_{\parallel}, k, \kappa, T)$ for the set $\{p_{\parallel}, k, \kappa, T\}$ values. These values at two different temperature are shown in Figure 3 as a function of k for all p_{\parallel} values. As mentioned in labels in figure, the data is shown for both bremsstrahlung and **aws** processes at two values of chemical potentials. As shown in Fig. 3, the p_{\parallel} and k dependence is very strong. The different colours in Fig. 3 show different baryon densities, temperatures and processes as mentioned in the figure. Further, there is only a weak dependence on κ for all the cases of baryon densities and fugacities used in the present work. We re-plot in Figure 4 these results versus the dynamical variable x . The data of various cases of Fig. 3 merge into a single curve similar to the Fig. 2. Therefore, the function g also depends only on the variable x , *i.e.*, $g(p_{\parallel}, k, \kappa, T) = g(x)$. It should be noted that this apparent single curve contains all the data for two temperatures, two baryon density values and two processes. Due to merging of all data in single curve, the other color symbols are overwritten and therefore are not visible. We parameterized the curves in Fig. 4 by fitting with polynomials ($g = \sum_n a_n x^n$) in the range of $x = 0.30 - 2.0$ and by a power law ($g = ax^b$) beyond as given by,

$$g(x) = 2.6709x^{0.4535460} \text{ for } x \leq 0.20$$

$$\begin{aligned}
g(x) &= \sum_{n=0}^4 a_n x^n \text{ for } 0.2 \leq x \leq 3.0 \\
g(x) &= \sum_{n=0}^5 b_n x^n \text{ for } 3.0 \leq x \leq 45.0 \\
g(x) &= 3.20816 \text{ for } x \geq 45.0
\end{aligned}$$

In above, $a_0 = 0.798609$, $a_1 = 2.44683$, $a_2 = -1.61357$, $a_3 = 0.551979$, $a_4 = -0.0720306$ and $b_0 = 2.31193$, $b_1 = 0.18221$, $b_2 = -0.0148997$, $b_3 = 0.584153E - 3$, $b_4 = -1.09125E - 5$, $b_5 = 7.79482E - 8$.

The purpose of rewriting Eq. 2 in the form of Eq. 7 is for the following reasons.

- (1) the $\int \frac{d^2\mathbf{p}_\perp}{(2\pi)^2} 2\tilde{\mathbf{p}}_\perp \cdot \Re\tilde{\mathbf{f}}(\tilde{\mathbf{p}}_\perp)$ of Eq. 2 above is very large extending over six orders of magnitude, whereas the $g(x)$ obtained by multiplying this with x^2 and the density dependent factors is reduced to just two orders of magnitude as shown on Fig. 4.
- (2) It separates the x dependent terms from the other terms in emission rate equations.
- (3) It is made to resemble Eq. 1. This implies that the new dimensionless emission function $g(x)$ replaces the dimensionless $J_T - J_L$ term of Eq. 1 in the presence of LPM effects. This emission function describes the photon emission of energy k , from quarks of momentum component p_\parallel and the physical conditions of the plasma, through a dimensionless dynamical variable x .
- (4) By empirical fits, the emission rates are reduced to one dimensional integrals similar to Eq. 1. Further, as discussed before, the full distributions are not very sensitive to chemical potentials and temperatures. Therefore, many of the properties of the dimensionless quantities $J_T - J_L$ may also be satisfied by the $g(x)$ function.²

The photon emission rates have been calculated for bremsstrahlung and **aws** using the empirical $g(x)$ functions for various values of μ . denoted by $\mathcal{R}_b, \mathcal{R}_a$ in Eq. 7. The emission rates for effective two loop processes without LPM effects have also been calculated using Eq. 1. As given in [9] the relative (normalized) suppression factors are given by,

$$S_b(k, \mu) = \left(\frac{\mathcal{R}_b}{\mathcal{R}_b^0} \right)_k \frac{f_b(\mu=0)}{f_b(\mu)} \quad \text{with} \quad f_b(\mu) = \left(\frac{\mathcal{R}_b}{\mathcal{R}_b^0} \right)_{k=20T} \quad (10)$$

$$S_a(k, \mu) = \left(\frac{\mathcal{R}_a}{\mathcal{R}_a^0} \right)_k \frac{f_a(\mu=0)}{f_a(\mu)} \quad \text{with} \quad f_a(\mu) = \left(\frac{\mathcal{R}_a}{\mathcal{R}_a^0} \right)_{k=0.2T} \quad (11)$$

These relative suppression factors are shown in Figure 5 for different (μ) quark chemical potentials for bremsstrahlung radiation at $T = 0.25\text{GeV}$. Figure 6 shows relative suppression factors for **aws** process. The relative suppression factors obtained from the rigorous calculations using variational method with eight trial functions are also shown in Figs.(5,6) by symbols. Figure 7 shows relative suppression factors for these two processes at $T = 0.55\text{GeV}$. It can be seen from Figs.(5-7) that the k/T of the x-axis is a good scale only for zero density case, *i.e.*, for different temperatures the zero density suppression curves are the same. However at finite density, the relative suppression factors depend on temperature. For example one may see the $\mu_q = 2.0\text{GeV}$ curve in Figs.(5,7). Using the present empirical method, we calculated the bremsstrahlung and **aws** suppression factors for the case of fugacities for quarks and gluons representing unsaturated phase space. These fugacities correspond to extreme cases of gluon dominated ($\lambda_g=0.10, \lambda_g/\lambda_q=10.0$) or quark dominated ($\lambda_g=0.01, \lambda_g/\lambda_q=0.1$) plasma. These results are in agreement with results from variational calculations for this case.

²This work was completed about a month back. However just few hours before putting on net, I noticed a paper on LPM effects in di-lepton sector by different method by Aurenche, Gelis, Moore and Zaraket. This will be studied later.

Conclusion

The photon emission rates from the quark gluon plasma have been studied considering LPM suppression effects at various temperatures and chemical potentials which represent the physical conditions of the plasma. Self-consistent iterations method and the variational method have been used to solve the AMY integral equation for the $\mathfrak{R}\tilde{\mathbf{f}}(\tilde{\mathbf{p}}_{\perp})$ distributions. The peak positions of these distributions from the variational method have been fitted by an empirical expression for various parameter sets. These peak positions are observed to be rather insensitive to the chemical potentials at all the temperatures considered. It is shown that the peak positions depend only on a new dynamical variable x rather than p_{\parallel} and k independently. Further, the integrated distributions multiplied by x^2 are shown to depend only on the variable x given by $g(x)$. This establishes that x is the only relevant dynamical variable for photon emission from QGP for these two processes. Empirical fits to the new $g(x)$ functions have been obtained. Using the empirical $g(x)$ functions, the relative suppression factors for bremsstrahlung and **aws** have been estimated as a function of photon energy for various chemical potentials. These suppression factors are shown to agree well with the rigorous results using variational method for all the cases studied. At finite density these bremsstrahlung and **aws** relative suppression factors versus k/T are temperature dependent.

Acknowledgements

I acknowledge the fruitful discussions with Drs. S. Kailas, A.K. Mohanty and A. Navin. My sincere thanks to the staff of computer division for computing facilities and co-operation during this study. My thanks to Dr. D.C. Biswas for making his personal computer available to me during this study.

References

- [1] Thomas Peitzman and Markus H. Thoma, hep-ph/0111114.
- [2] P. Aurenche, F. Gelis, H. Zaraket and R. Kobes, Phys. Rev. **D58** 085003 (1998), [hep-ph/9804224] ;
P. Aurenche, F. Gelis, R. Kobes and E. Petitgirard, Phys. Rev. **D54** 5274 (1996) [hep-ph/9604398]; Z. Phys. **C75**,315 (1996).
- [3] P. Aurenche, F. Gelis, R. Kobes and H. Zaraket, Phys. Rev. **D61** 116001 (2000) [hep-ph/9911367]
- [4] P. Aurenche, F. Gelis, and H. Zaraket, Phys. Rev. **D62** 096012 (2000) [hep-ph/0003326]
- [5] P. Aurenche, F. Gelis, and H. Zaraket, hep-ph/0204146
- [6] Peter Arnold, Guy D. Moore and Laurence G. Yaffe, JHEP 0112 (2001) 009, [hep-ph/0111107]
- [7] Peter Arnold, Guy D. Moore and Laurence G. Yaffe, JHEP 0111 (2001) 057, [hep-ph/0109064].
- [8] Peter Arnold, Guy D. Moore and Laurence G. Yaffe, hep-ph/0204343.
- [9] S. V. S. Sastry, hep-ph/0208103.

$T = 0.25$						$T = 0.35$			
μ	κ	$J_T - J_L$	f_b	f_a		κ	$J_T - J_L$	f_b	f_a
0.00	0.25000	2.05215	0.85500	1.00000		0.25000	2.05215	0.85500	1.00000
0.25	0.25589	2.02793	0.83813	0.99791		0.25311	2.03926	0.84595	0.99888
0.50	0.26943	1.97486	0.80245	0.99351		0.26119	2.00672	0.82397	0.99612
0.75	0.28385	1.92201	0.76243	0.98939		0.27156	1.96682	0.79697	0.99287
1.00	0.29572	1.88105	0.72491	0.98637		0.28190	1.92892	0.76926	0.98991
1.50	0.31102	1.83136	0.65706	0.98293		0.29855	1.87162	0.71568	0.98570
2.00	0.31912	1.80636	0.59987	0.98129		0.30940	1.83649	0.66820	0.98327
$T = 0.45$						$T = 0.55$			
0.00	0.25000	2.05215	0.85500	1.00000		0.25000	2.05215	0.85500	1.00000
0.25	0.25191	2.04421	0.84940	0.99931		0.25129	2.04678	0.85122	0.99953
0.50	0.25715	2.02283	0.83485	0.99748		0.25492	2.03184	0.84097	0.99824
0.75	0.26452	1.99366	0.81551	0.99504		0.26032	2.01017	0.82653	0.99641
1.00	0.27274	1.96239	0.79439	0.99252		0.26673	1.98514	0.80995	0.99434
1.50	0.28815	1.90691	0.75176	0.98826		0.28009	1.93542	0.77486	0.99041
2.00	0.30001	1.86678	0.71166	0.98536		0.29177	1.89445	0.74034	0.98734
$T = 0.55$									
1.00	0.25000	2.05215	0.85500	1.00000					
0.10	0.31850	1.80824	0.85782	0.98141					
10.0	0.22898	2.14498	0.88409	1.00848					
5.00	0.23494	2.11758	0.88153	1.00590					

Table 1: Normalization factors as a function of baryon density represented by quark chemical potential (in GeV) for various temperatures (in GeV). The κ value used in the integral equation and the J_T, J_L values required are also given in Table. The last four entries of Table are for unsaturated plasma for the parameters in text, with the second column for λ_g/λ_q .

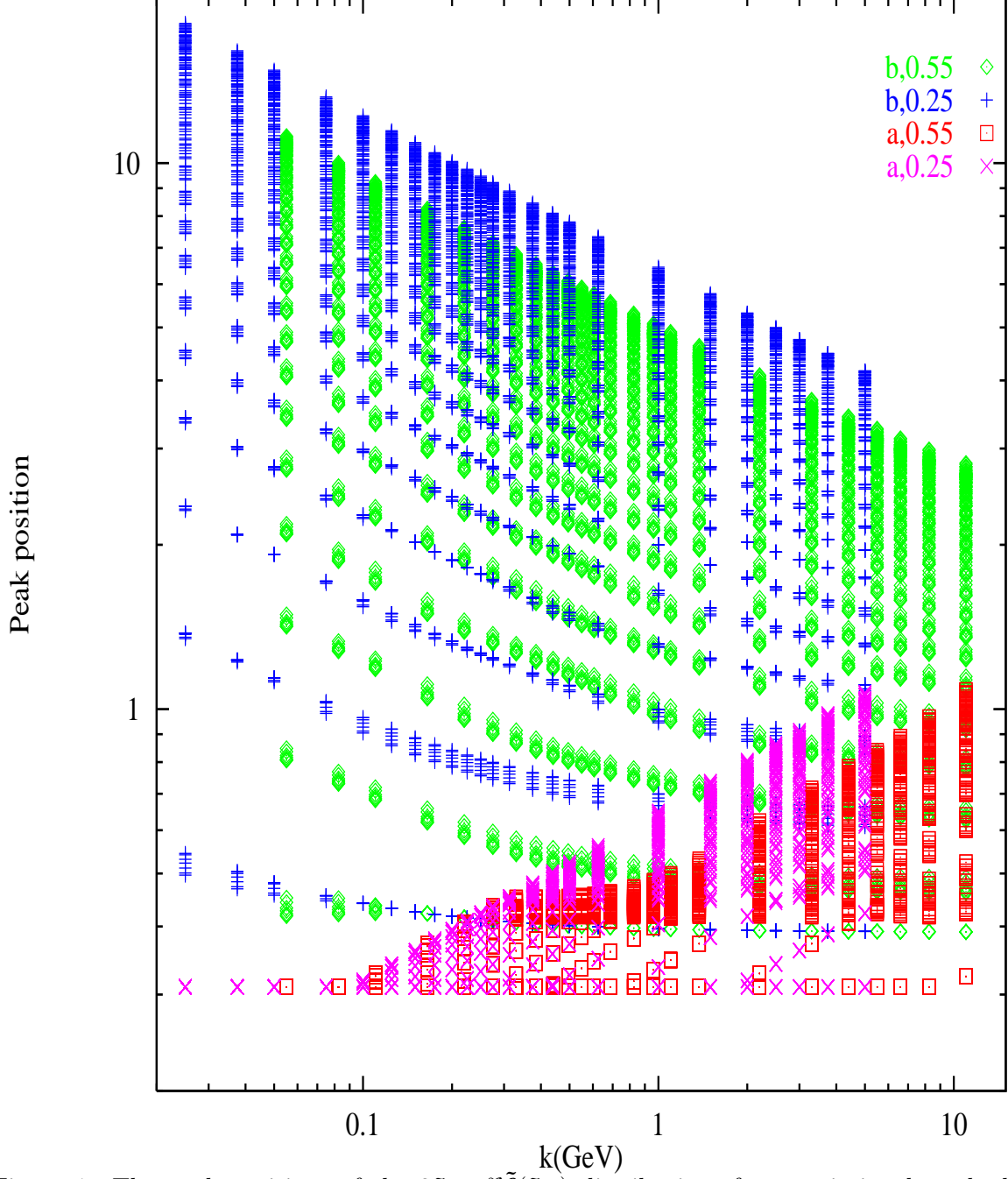


Figure 1: The peak positions of the $2\tilde{\mathbf{p}}_{\perp} \cdot \mathfrak{R}\tilde{\mathbf{f}}(\tilde{\mathbf{p}}_{\perp})$ distributions from variational method for bremsstrahlung and **aws** processes versus photon energy. The data is shown for two temperatures. For each process at a given temperature, the data contains (7x24 points) seven baryon density values and twenty four p_{\parallel} values all in same symbol and color.

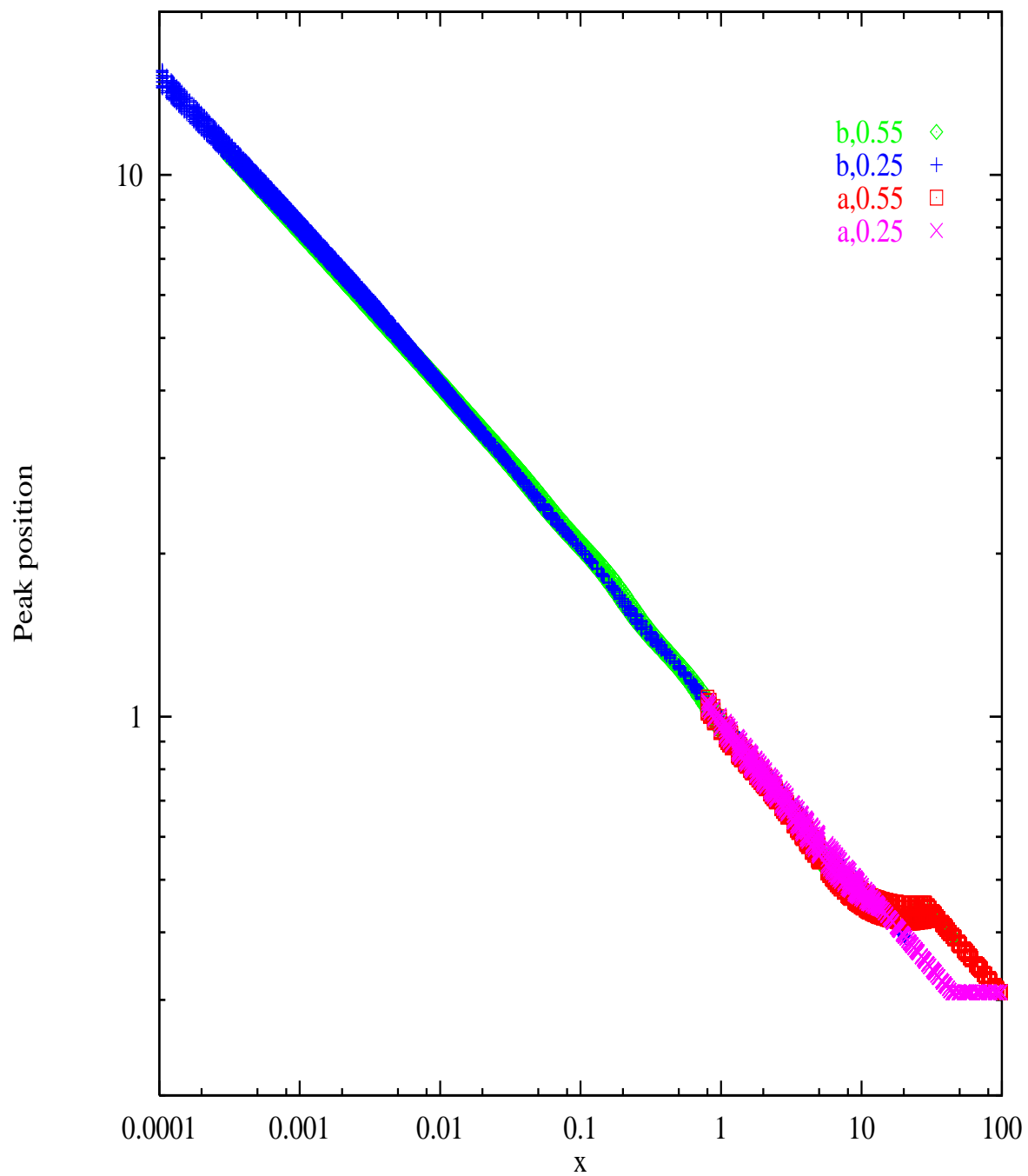


Figure 2: Same as Fig. 1 but plotted versus new dynamical variable x .

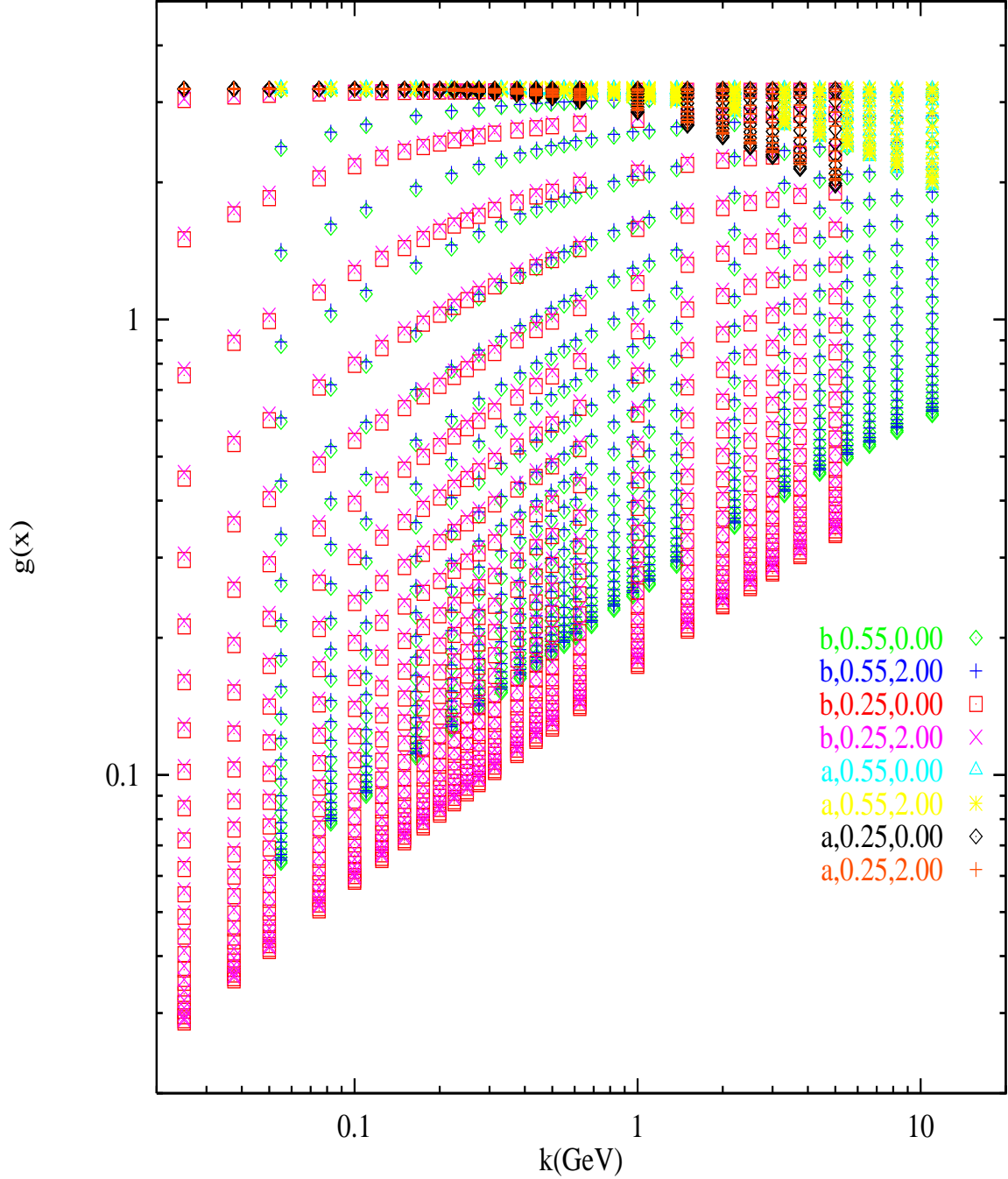


Figure 3: The new dimensionless emission function $g(k, p_{\parallel}, \kappa, T)$ mentioned in the text versus photon energy. This data is generated from the variational method for bremsstrahlung and **aws** processes and shown by labels b and a in figure. The labels in figure show process, temperatures and chemical potential values. For each process at a given temperature and density values, the data contains several p_{\parallel} values all in same symbol and color.

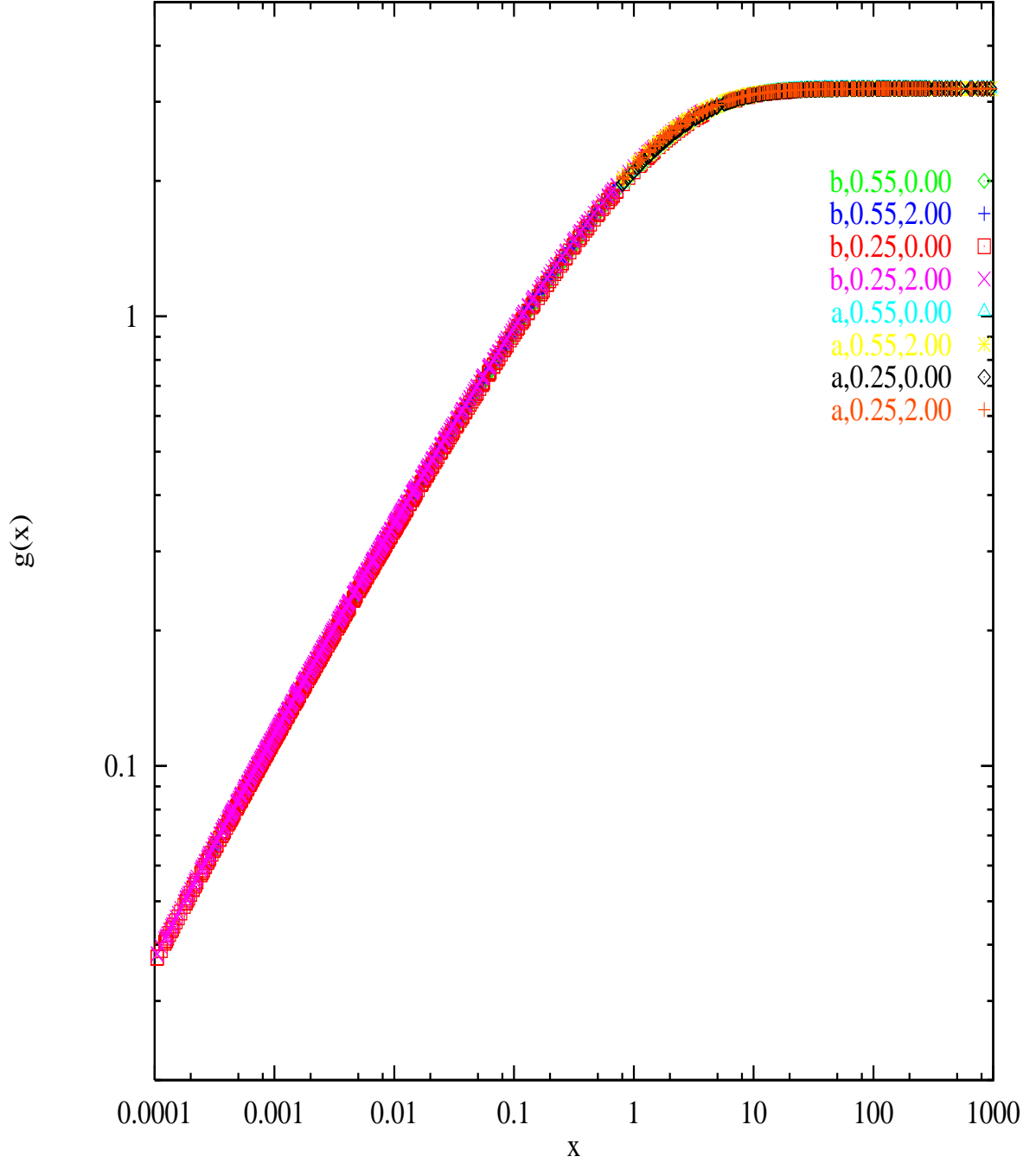


Figure 4: Same as Fig.3, the new dimensionless emission function $g(x)$ versus dynamical variable x . All the cases of Fig. 3 are in the figure but may not be visible due to superposition of various symbols.

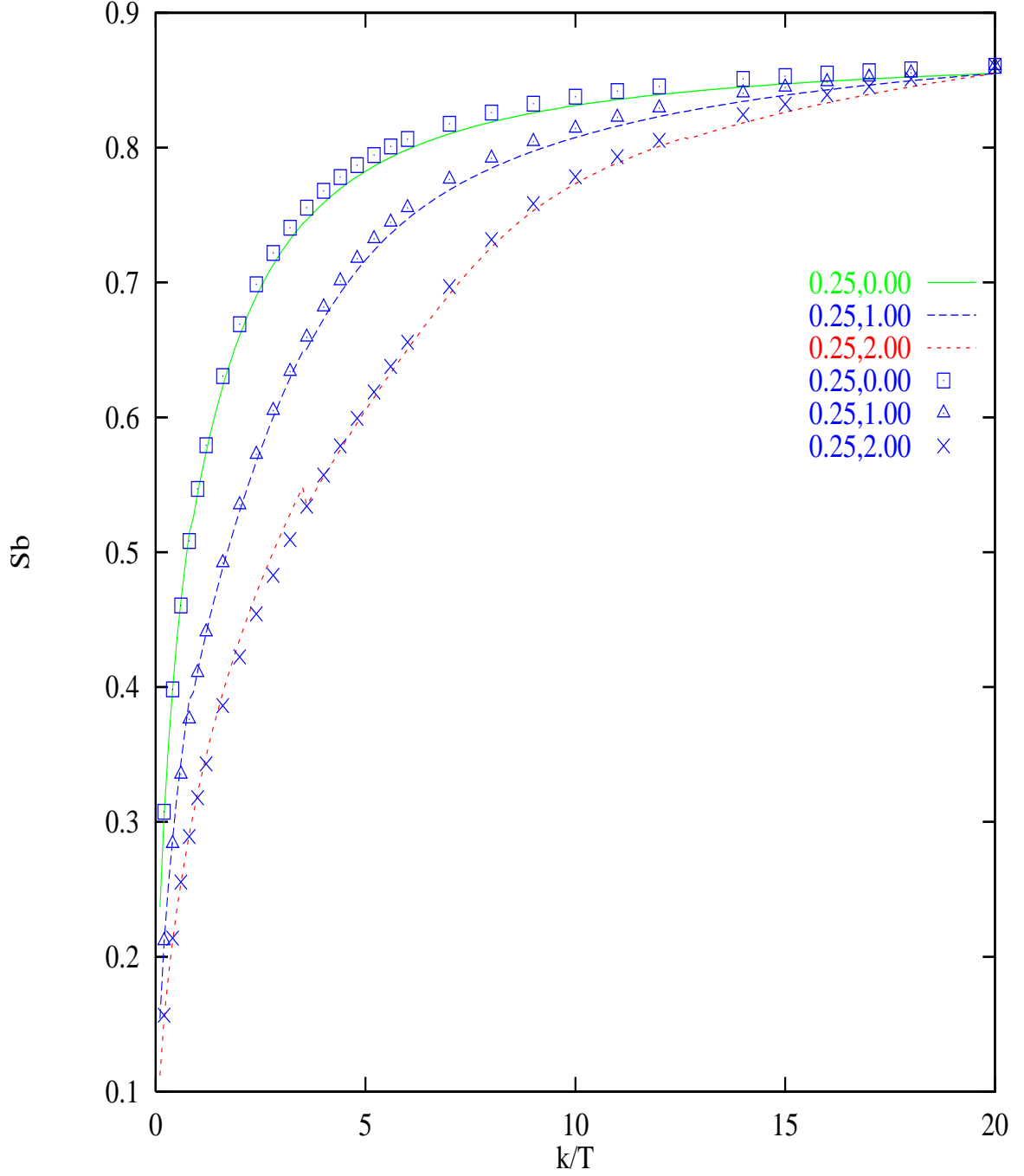


Figure 5: Suppression factors for bremsstrahlung radiation relative to zero density case. The temperature is 0.25GeV and chemical potential values are mentioned in the figure. The curves are obtained from the empirical $g(x)$ function, and the symbols are from rigorous results using variational method with $n_r = 8$.

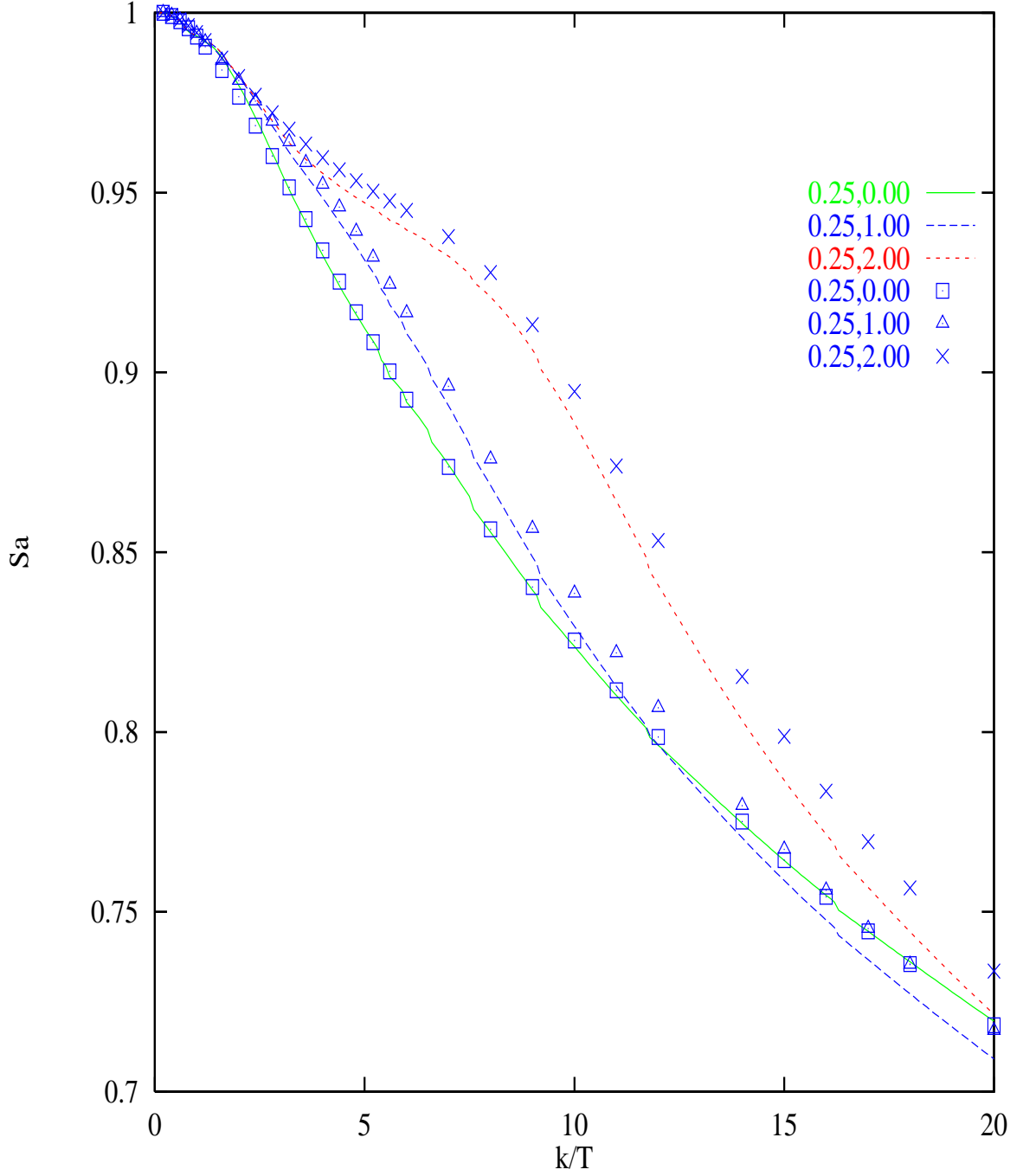


Figure 6: Suppression factors for radiation from **aws** relative to zero density case. The temperature is 0.25GeV and the chemical potential values are mentioned in the figure. The curves are obtained from the empirical $g(x)$ function, and the symbols are from rigorous calculations using variational method with $n_r = 8$.

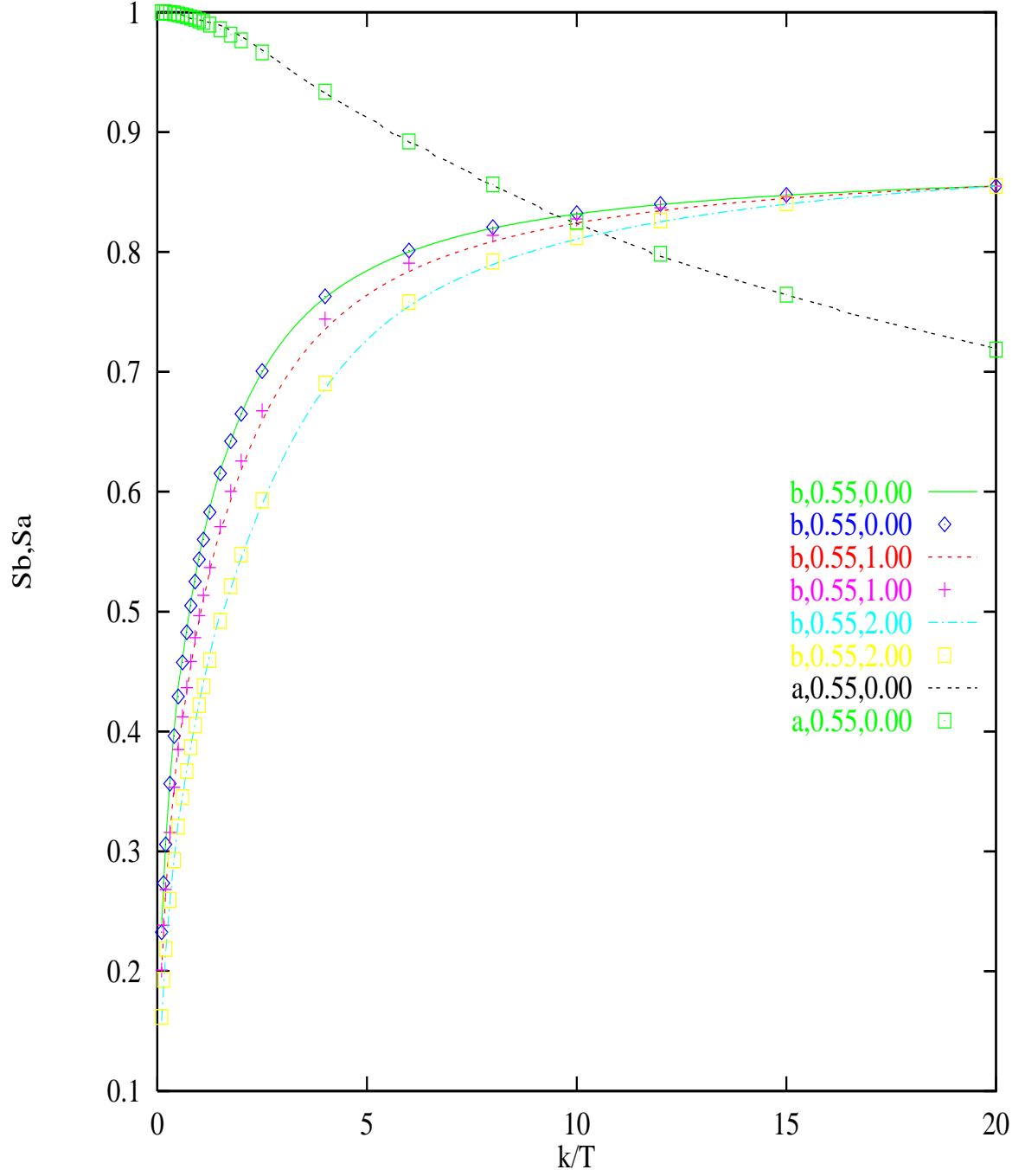


Figure 7: Suppression factors for bremsstrahlung and **aws** radiation relative to zero density case. The temperature is 0.55GeV and chemical potential values are mentioned in the figure. The curves are obtained from the empirical $g(x)$ function, and the symbols are from rigorous results using variational method with $n_r = 8$.

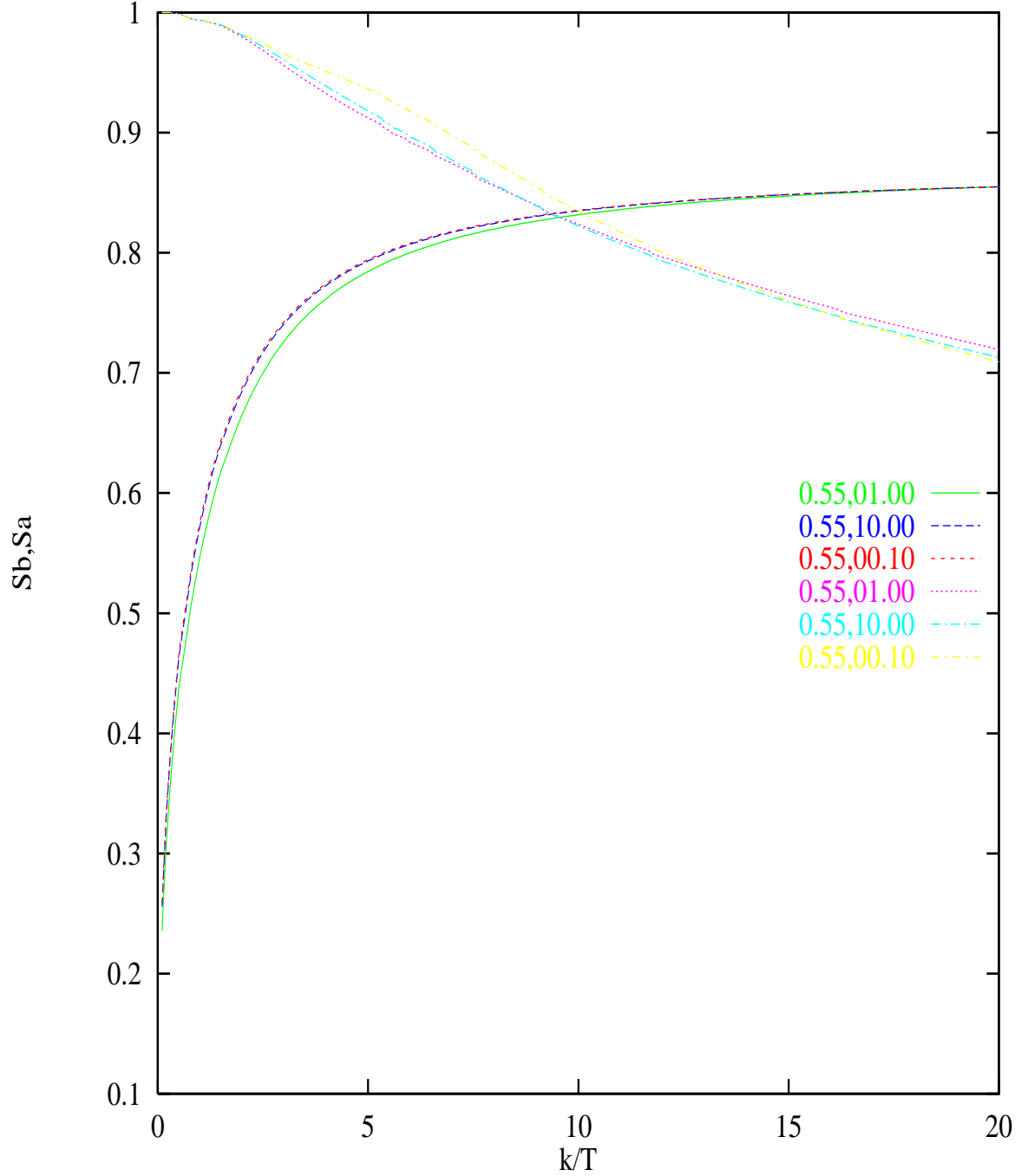


Figure 8: Suppression factors for bremsstrahlung and **aws** radiation relative to saturated plasma, represented by labels **b** and **a** . The temperature is 0.55GeV and the λ_g/λ_q values are mentioned in the figure. The curves are obtained from the empirical $g(x)$ function.